Collective plasma response of interacting electrons localized in disordered $GaAs/Al_xGa_{1-x}As$ superlattices

Yu. A. Pusep,[1] W. Fortunato,[1] P. P. González-Borrero,[2] A. I. Toropov,[3] and J. C. Galzerani[1]
[1]*Departamento de Fisica, Universidade Federal de São Carlos, Caixa Postal 676, 13565-905 São Carlos, Brazil*
[2]*Instituto de Fisica de São Carlos, Universidade de São Paulo, 13560-970 São Carlos, São Paulo, Brazil*
[3]*Institute of Semiconductor Physics, 630090 Novosibirsk, Russia*
(Received 16 March 2000; revised manuscript received 18 August 2000; published 1 March 2001)

The collective plasmon-LO phonon excitations were studied by Raman scattering in intentionally disordered GaAs/AlGaAs superlattices with various strengths of disorder. The results were compared with the data obtained in the differently doped superlattices where the fixed disorder was mainly provided by the monolayer fluctuations of the layer thicknesses. Thus, the influences of both disorder and electron-electron interaction on the behavior of localized electrons were explored. We found that in the presence of disorder, the collective excitations tend to form coherently oscillating clusters with a finite extent. It was shown that while interaction causes the formation of coherent clusters, the effect of both the temperature and disorder is to destroy them; these evolutions of the clusters revealed a critical behavior.

DOI: 10.1103/PhysRevB.63.115311 PACS number(s): 72.15.Nj, 71.55.Jv

I. INTRODUCTION

The problem of interacting electrons in disordered potential attracted much attention soon after the importance of Coulomb electron–electron interaction in the metal-to-insulator transition was realized.[1–3] This problem is strongly connected with the transport properties of electrons in disordered systems; however, the interplay between disorder and interaction influences the high frequency (optical) response of electrons as well. As a matter of fact, the electron–electron interaction plays a determinative role in the collective plasma oscillations which take place at a resonant plasma frequency ω_p. Therefore, it is clear that the reaction of the disordered electron system to a field of electromagnetic radiation with a frequency ω_p provides a staightforward way to probe the effects of interaction and disorder.

It is well known, that free electrons reveal a plasma resonance at the frequency $\omega_p = \sqrt{4\pi e^2 N/m}$, where e, N, and m are the charge, the concentration and the mass of electrons, respectively. In perfect crystals the plasma oscillations have the form of plane waves spreading over the whole crystal volume. Certainly, disorder should destroy the collective plasma oscillations reducing the coherency length of the plasmons and thus, giving rise to their localization. However, as it has been shown in Refs. 4 and 5, even in the presence of disorder, at least part of the electrons will find resonance conditions adapting their phases and forming the coherently oscillating spatial clusters. As a result, the natural inhomogeneous broadening of a disordered system can be completely screened out by the dynamical many-particle interaction of the coherent electrons, causing a narrowing of the spectral lines associated with the electron excitations.

Recently, the spectral properties of the strongly correlated 3D disordered system have been considered in Ref. 6 where similar results were obtained; namely, it was shown that the interaction causes the band narrowing and a redshift.

As it has been discussed in Refs. 1 and 2 the behavior of the interacting electrons in the presence of disorder is determined by the ratio U/Δ, where U denotes the interaction strength, while Δ is the disorder strength. This ratio defines the localization length of the interacting electrons, which was shown to increase as interaction increases and disorder decreases.

In order to investigate the collective response of the interacting localized electrons, Raman scattering, the most powerful method to study the low-energy excitations in solids, can be applied. It is worth mentioning, that the collective excitations were broadly studied in semiconductor superlattices by Raman scattering.[7] However, to our best knowledge, a study of the collective plasmalike excitations in the presence of disorder yet was not performed.

We already showed that Raman scattering serves as a tool to probe both the spatial (the coherence length) and the energy (the resonance frequency and the damping) characteristics of the collective excitations in disordered semiconductors, where the Raman selection rules are relaxed resulting in a specific asymmetry of the Raman lines associated with the collective excitations.[8,9]

In this paper we use the results obtained in Refs. 8 and 9 to study the collective reaction of electrons subjected to the random potential of the semiconductor superlattices, where both the localization and the strength of the electron–electron interaction can be controlled by the growth. Here disorder was introduced by a controlled random variation of the well thicknesses, while the interaction was changed by the different doping.

It was shown that, as predicted by the theory,[4,5] in the presence of disorder the interacting electrons form coherent clusters with finite spatial extents. These clusters revealed an unexpected critical behavior with the variation of the temperature and interaction similar to the critical behavior of the spontaneously polarized domains in ferroelectrics. It was found that increasing disorder causes the decrease of the size of the coherent clusters accompanied by the increase in their inhomogeneities.

The paper is organized as follows. A theoretical analysis

of the collective excitations in disordered semiconductor superlattices and their contribution to Raman scattering is briefly presented in Sec. II. In Sec. III we describe the experimental details. The experimental results together with their discussion are given in Sec. IV, while conclusions are outlined in Sec. V.

II. THEORY

In the presence of disorder, collective excitations can be represented as a superposition of plane waves with the wave vectors distributed in a finite interval of the wave function uncertainty $\delta\mathbf{q}$. In this case, according to the model successfully used for the optical phonons in microcrystalline silicon[10] one can present the wave function in a form of a Gaussian:

$$\psi(\mathbf{r}) = \frac{1}{\sqrt{\pi L_c}} \exp\left(- \frac{2\mathbf{r}^2}{L_c^2} \right) \tag{1}$$

which means the effective localization at $|\mathbf{r}| \lesssim L_c$. Expanding (1) in a Fourier integral we obtain

$$\psi(\mathbf{r}) = \int d^3q \, C(\mathbf{q}) \exp(i\mathbf{q}\mathbf{r}) \tag{2}$$

with

$$C(\mathbf{q}) = \frac{1}{(2\pi)^3} \int d^3r \, \psi(\mathbf{r}) \exp(-i\mathbf{q}\mathbf{r}).$$

The values of the Fourier coefficients $C(\mathbf{q})$ can be calculated using (1):

$$C(\mathbf{q}) = \frac{1}{\pi^2 \sqrt{2L_c}} \exp\left(- \frac{\mathbf{q}^2 L_c^2}{8} \right). \tag{3}$$

As a result, the wave function $\psi(\mathbf{r})$ is represented as a superposition of eigenfunctions of the type of 3D plane waves with the wave vectors $\mathbf{q}$ distributed in the interval $|\delta\mathbf{q}| \lesssim 1/L_c$. These eigenfunctions are weighted through the coefficients $C(\mathbf{q})$ according to a Gauss distribution. This implies that the excitations with wave vectors in the above determined interval $\delta\mathbf{q}$ can be excited by Raman scattering (when $\mathbf{q} \simeq 0$) with the probability $|C(\mathbf{q})|^2$. Then, the Raman intensity can be written in the following form:[8]

$$I(\omega) \sim \int |C(\mathbf{q})|^2 f_{sc}(\mathbf{q}) \frac{d^3q}{[\omega - \omega_{\mathrm{exc}}(\mathbf{q})]^2 + (\Gamma/2)^2}$$
$$\sim \int f_{\mathrm{sc}}(\mathbf{q}) \exp\left(- \frac{\mathbf{q}^2 L_c^2}{8} \right) \frac{d^3q}{[\omega - \omega_{\mathrm{exc}}(\mathbf{q})]^2 + (\Gamma/2)^2}, \tag{4}$$

where $f_{\mathrm{sc}}(\mathbf{q}) = [4\pi/(q^2 + q_0^2)]^2$ is the screening correlation function (here q_0 is the screening wave vector).

It is clear that the excitations allowed in the interval of wave vectors $\delta\mathbf{q}$ will contribute to the Raman intensity at frequencies determined by their dispersions $\omega_{\mathrm{exc}}(\mathbf{q})$. It is worth reminding, that the localization length L_c is associated with the spatial extent of the wave function, whereas the damping constant Γ is caused by the energy losses contributes to the relaxation process.

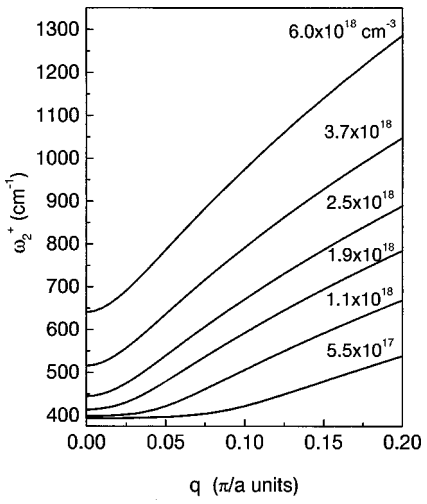

FIG. 1. Dispersions of the AlAs-type collective coupled plasmon-LO phonon excitations calculated by RPA in the $(GaAs)_{17}(AlAs)_2$ superlattices with different electron densities.

The Raman intensity defined in such a way was used to fit the experimental spectra and thus, to obtain the characteristic parameters of the collective excitations of interest.

In the doped GaAs/AlGaAs superlattices here studied, the Coulomb coupling between the plasmons and the LO phonons give rise to three coupled collective plasmon-LO phonon modes: a low-frequency acousticlike mode (ω^-) and two high-frequency optic GaAs-type (ω_1^+) and AlAs-type (ω_2^+) ones, respectively. The AlAs-type coupled modes were shown to have an essentially plasmonlike character already at rather low electron concentrations,[9] what allows them to be easily analyzed; therefore, we focused our analysis to these modes.

The dispersions of the ω_2^+ modes calculated by the random phase approximation (the details can be found in Ref. 9) in the superlattices with different electron densities are plotted in Fig. 1. As it was discussed above, all the collective states distributed in a finite interval $\delta\mathbf{q}$ contribute to the Raman process in disordered superlattice. Depending on the electron concentration and on the coherence length, this produces different widths of the asymmetrical Raman lines calculated by (4), which are shown in Fig. 2. It is worth adding, that as it is seen from Fig. 1, the parabolic approximation is not valid at low electron densities for wave numbers very close to the center of the Brillouin zone, where the frequency approximates its own value at $q = 0$. Therefore, very different widths of the Raman lines can result in similar values of $\delta\mathbf{q}$ and, as a consequence, a similar values of L_c can be obtained in the samples with different electron densities.

III. EXPERIMENT

In our previous paper[9] we explored the short period $(GaAs)_{17}(AlAs)_2$ superlattices (where the numbers denote

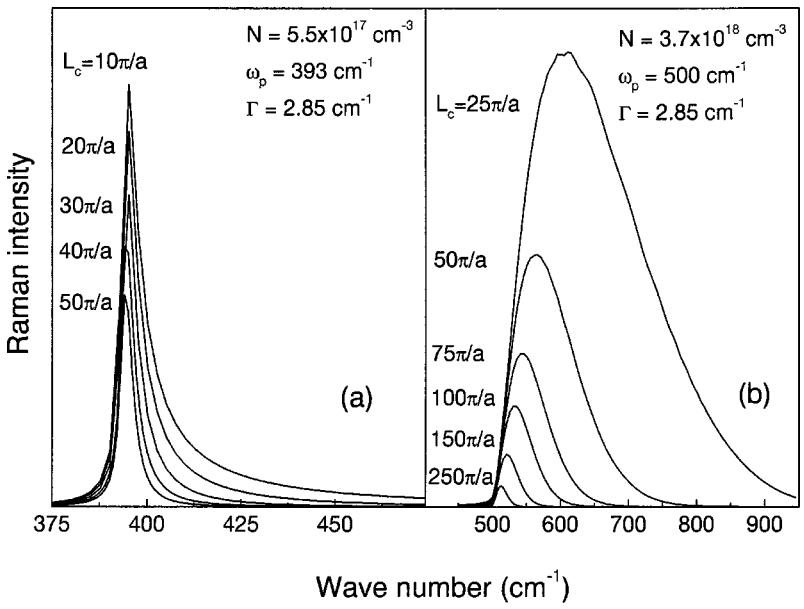

FIG. 2. Intensities of the Raman lines associated with the AlAs-type coupled excitations with different values of the coherence lengths (L_c) calculated in the $(GaAs)_{17}(AlAs)_2$ superlattices with the electron densities $N=5.0\times10^{17}\,cm^{-3}$ and $N=3.7\times10^{18}\,cm^{-3}$.

the thicknesses of the corresponding layers expressed in monolayers) doped with Si. According to the calculations made by the envelope function approximation, these superlattices reveal a lowest broad miniband with a width $W\approx65$ meV, while the unavoidable monolayer fluctuations of the layer thicknesses produce fluctuations of the noninteracting electron energies distributed in the energy interval $\Delta E\approx12$ meV. The natural monolayer fluctuations result in the electron localization.[11] Evidences of the electron localization in the superlattices under investigation were obtained by the measurements of the thermostimulated current[12] and the capacitance.[13] Such a localization is the intrinsic property of the superlattices and its strength should not be different for the superlattices grown in the same conditions. Therefore, we expect that at not very high doping levels different doping will change the strength of the electron–electron interaction, while fixing a strength of disorder. Certainly, heavy doping should result in an additional ''impurity disorder.''

In order to control the strength of disorder the $(GaAs)_m(Al_{0.3}Ga_{0.6}As)_6$ superlattices were prepared with a fixed doping. The vertical disorder was produced by the controlled random variation of the GaAs well thicknesses around the nominal value $m=17$ ML corresponding to a Gauss distribution of the lowest levels of noninteracting electrons forming the conduction miniband, while the barrier thicknesses were unchanged. The samples were grown by molecular beam epitaxy on (100) oriented GaAs substrates. In order to avoid the short-range in-plane fluctuations, the growth of the superlattices was interrupted for 20 s at the normal interface and for 3–5 s at the inverted one. The total number of 50 periods was grown. The strength of disorder was characterized by the disorder parameter $\delta=\Delta/W$, where Δ is the full width at half-maximum of a Gauss distribution of the energy of the noninteracting electrons calculated in the isolated quantum well and W is the width of the nominal miniband in the absence of disorder. In the above-mentioned superlattices the monolayer fluctuations produce $\delta\approx0.18$. The values of the dopings were calibrated during the growth of the doped equivalent $Al_{0.11}Ga_{0.89}As$ alloys [the alloy with the same contents of Al as in the relevant $(GaAs)_{17}(AlAs)_2$ superlattice]. In the following, we will use the nominal values of the doping concentration of Si as the concentration of electrons. For relatively low doped superlattices (those with the nominal doping concentration less than $2\times10^{18}\,cm^{-3}$) the Hall concentrations were smaller than the nominal ones, while in the heavily doped samples their difference was found inside the experimental error. This difference is clearly seen in the Hall data presented in Figs. 8 and 9 for two superlattices with the nominal doping concentrations $7.0\times10^{17}\,cm^{-3}$ (Fig. 8) and $2.5\times10^{18}\,cm^{-3}$ (Fig. 9). In addition, as it is seen from these figures, the mobility of electrons was higher in the sample with higher doping level where the Fermi level is expected to lie above the fluctuations of the electron potential. The differences between the nominal doping levels and the Hall concentrations together with the low mobilities observed in low doped superlattices are the additional evidences of localization.

The back scattered Raman spectra were performed with a ''Instruments S.A. T64000'' triple grating spectrometer supplied with a CCD detector cooled by liquid nitrogen. The 5145 Å line of an Ar^+ laser was used for excitation. In order to perform the measurements at different temperatures the samples were mounted in a ''Janis CCS-150'' closed circle helium cryostat.

In the superlattices, because of the conservation of the momenta in the Raman process, we probed the vertically polarized coupled modes which have their origins in the intraminiband plasmons. The data obtained in the superlattices with different electron concentrations and with a fixed disorder were compared with those measured in the superlattices with various strength of disorder and with a fixed electron density.

IV. RESULTS AND DISCUSSION

The typical Raman spectrum measured in the $(GaAs)_m(Al_{0.3}Ga_{0.6}As)_6$ superlattice with the disorder pa-

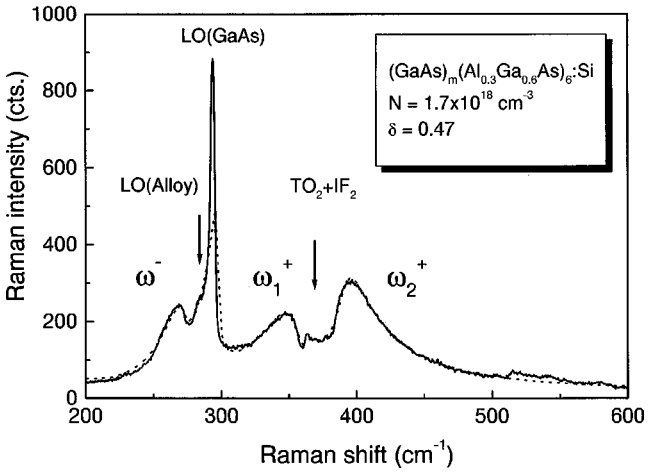

FIG. 3. Raman spectra of the $(GaAs)_m(Al_{0.3}Ga_{0.7}As)_6$ superlattice with the electron concentration $N=1.7\times10^{18}\,cm^{-3}$ and the parameter of disorder $\delta=0.47$ measured at $T=10$ K. The dotted line is the spectrum calculated as explained in the text.

rameter $\delta=0.47$ and the electron concentration $N=1.7\times10^{18}\,cm^{-3}$ is shown in Fig. 3 together with the spectrum calculated by Eq. (4). The lines due to the GaAs-type optical phonons (LO_1) and the AlAs-type ones (TO_2 and the interface modes IF_2) together with the coupled plasmon-LO phonon collective modes were clearly detected. The different characters of the coupled modes, the phononlike for the GaAs-type one and the plasmonlike for the AlAs-type one are responsible for their different asymmetries.[9] Further, we present the data concerning the AlAs-type mode.

Some selected Raman spectra of the GaAs/AlGaAs superlattices with a fixed disorder and different electron concentrations and with a fixed electron concentration and varied disorder are demonstrated in the frequency range of the AlAs-type optical phonons in Figs. 4 and 5, respectively. The formation of the strongly asymmetrical Raman lines associated with the collective coupled excitations in disordered superlattices is clearly seen in these figures. The dotted lines present the results of the fittings using Eq. (4). The values of the parameters determining the shapes of the relevant Raman lines are collected in Figs. 6 and 7.

A. Dependence on electron density (strength of interaction). Fixed disorder

The Raman spectra relevant to this case are shown in Fig. 4. The values of the broadenings Γ, the positions of the AlAs-type plasmon-LO phonon Raman lines ω_2^+ and the values of the coherence lengths L_c associated with the spatial localization of the collective excitations, obtained by the fitting of the intensities calculated by the expression (4) to the experimental spectra, are plotted in Figs. 6(a)–6(c). For a comparison, the dependence of the frequency of the AlAs-type plasmon-LO phonon excitations at the center of the Brillouin zone on the electron concentration calculated for the case when the line shift is determined by the occupation of the miniband of the perfectly ordered superlattice is shown in Fig. 6(b) by the solid line. These calculations were

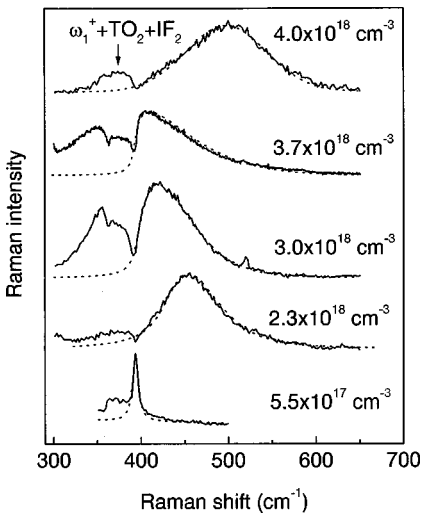

FIG. 4. Raman spectra of the AlAs-type collective coupled excitations measured at $T=10$ K in the $(GaAs)_{17}(AlAs)_2$ superlattices with different electron densities and a fixed disorder ($\delta=0.18$). The dotted lines show the calculated contributions of the AlAs-type excitations.

made according to the theory presented in Ref. 14, where the finite width of the miniband was taken into account.

In the sample with the lowest doping ($N=5\times10^{17}\,cm^{-3}$) the AlAs-type optical mode presents a mostly phononlike character and it reveals a Lorentzian shape characterized by the homogeneous broadening $\Gamma=3.5\,cm^{-1}$. With the increase of the doping level, as a consequence of the plasmon-LO phonon interaction, this line shifts to the high frequencies, increases in intensity, and its shape acquires a strong asymmetry. Meanwhile, the broadening Γ rises with the increase of the electron density, caused by the increase of the disorder induced by the random

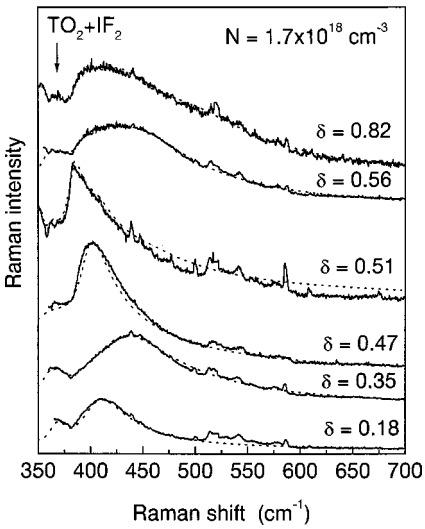

FIG. 5. Raman spectra of the AlAs-type collective coupled excitations measured at $T=10$ K in the $(GaAs)_m(Al_{0.3}Ga_{0.7}As)_6$ superlattices with different parameters of disorder and a fixed electron density ($N=1.7\times10^{18}\,cm^{-3}$). The dotted lines show the results of the fitting.

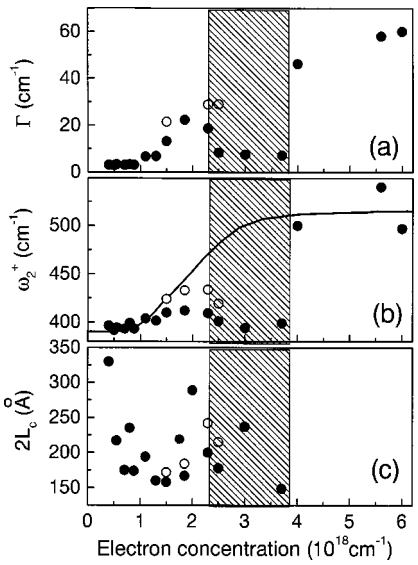

FIG. 6. Dependencies of the damping constant (Γ), the frequency (ω_2^+), and the coherence length (L_c) of the AlAs-type collective plasmon-LO phonon excitations on the electron density measured at $T=10$ K in the $(GaAs)_{17}(AlAs)_2$ superlattices with a fixed disorder ($\delta=0.18$).

impurity potential, which acts as a reason for the scattering of the plasmon-type excitations. However, a strong line narrowing accompanied by a pronounced redshift was found beginning with the electron concentration $N=2.5\times10^{18}\,\mathrm{cm}^{-3}$.

According to the theory presented in Ref. 4–6 the coherent collective response of interacting localized electrons is responsible for the observed spectral narrowing. At low electron densities, the long distances between electrons do not allow an effective interaction between them. By increasing the electron densities, the cooperative behavior of the interacting electrons becomes dominating, resulting in the formation of a strongly correlated electron plasma in the presence of disorder, when the dynamical many-particle interaction almost completely screens out the effects of the random potential fluctuations. As a consequence, the broadenings Γ acquire the values very close to those found in the low-doped samples. The line narrowing was observed at the critical electron density $N_c=2.3\times10^{18}\,\mathrm{cm}^{-3}$ corresponding to the value of the ratio of the energy of the electron–electron interaction and the Fermi energy $r_s\equiv E_{ee}/E_F\approx0.2$, which means a regime of intermediate interaction.

With a further increase of the doping, an abrupt increase of both the line broadening and the spectral line shift was observed at $N=4.0\times10^{18}\,\mathrm{cm}^{-3}$. At such high electron concentrations the impurity disorder becomes very strong; this breaks down the correlation responsible for the line narrowing and the collective excitations turn out to be strongly damped. Now, the broadening Γ dominates resulting in a symmetrical shape of the plasmon-LO phonon line, and its value and the value of the characteristic frequency ω_2^+ return to those values relevant to a perfectly ordered superlattice [see Figs. 6(a) and 6(b)].

A decrease of the coherence length L_c with the increase of the electron concentration was observed in the samples with low doping levels, where the electron–electron interaction is still weak and the impurities are responsible for the spatial limitation of the collective excitations. However, in the range where the correlation effects were detected (the hatched areas in Fig. 6), L_c reveals a tendency to increase—the effect predicted in Refs. 1 and 2 for the interacting localized electrons.

The double data shown in Fig. 6 for some of the samples (the closed and opened circles) mean that the Raman lines associated with the collective excitations could not be fitted well with a single line calculated by formula (4). This implies that the nonuniformity of the correlated clusters appear when approximating the critical value of the electron density.

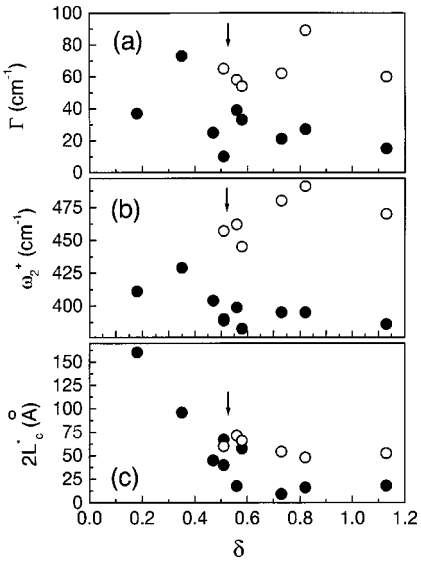

FIG. 7. Dependencies of the damping constant (Γ), the frequency (ω_2^+), and the effective coherence length (L_c^*) of the AlAs-type collective plasmon-LO phonon excitations on the parameter of disorder measured at $T=10$ K in the $(GaAs)_m(Al_{0.3}Ga_{0.7}As)_6$ superlattices with a fixed electron density ($N=1.7\times10^{18}\,\mathrm{cm}^{-3}$).

B. Dependence on the strength of disorder. Fixed electron density

When the samples have a fixed density of electrons, the dispersion of the collective excitations calculated by the random phase approximation (RPA) is not changed from one sample to another. Thus, the increase of the asymmetrical broadening of the Raman lines observed with the increase of the disorder (see Fig. 5) can be completely attributed to the decrease of the corresponding coherence length. However, up to which strength of disorder (and accompanying localization) the RPA is valid is not yet clear. Therefore, we interpreted the values of the coherence lengths obtained in the intentionally disordered superlattices as the ''effective coherence lengths'' (L_c^*).

The parameters characterizing the collective excitations of interest are depicted in Fig. 7. Surprisingly, the effect of the line narrowing was found even with the alteration of disorder around $\delta=0.4$. However, with the further increase of disor-

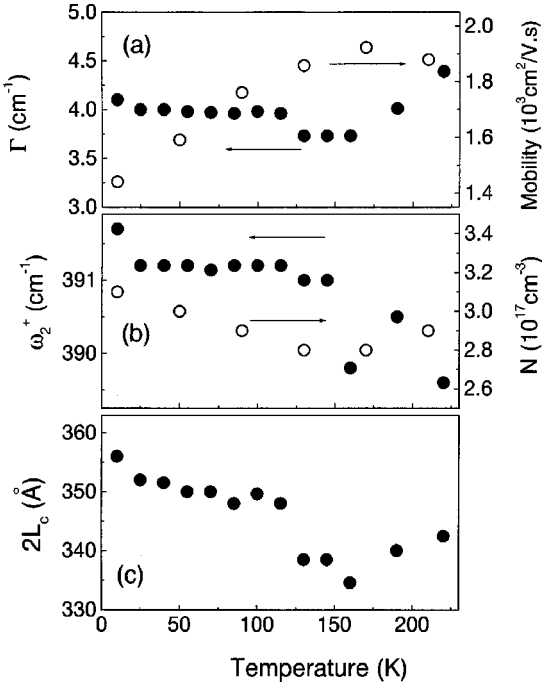

FIG. 8. Temperature dependencies of the damping constant (Γ), the frequency (ω_2^+), and the coherence length (L_c) of the AlAs-type collective plasmon-LO phonon excitations measured in the $(GaAs)_{17}(AlAs)_2$ superlattices with the electron density $N=7.0\times10^{17}\,cm^{-3}$ ($\delta=0.18$). The electron mobilities and concentrations measured by Hall effect are shown by open circles.

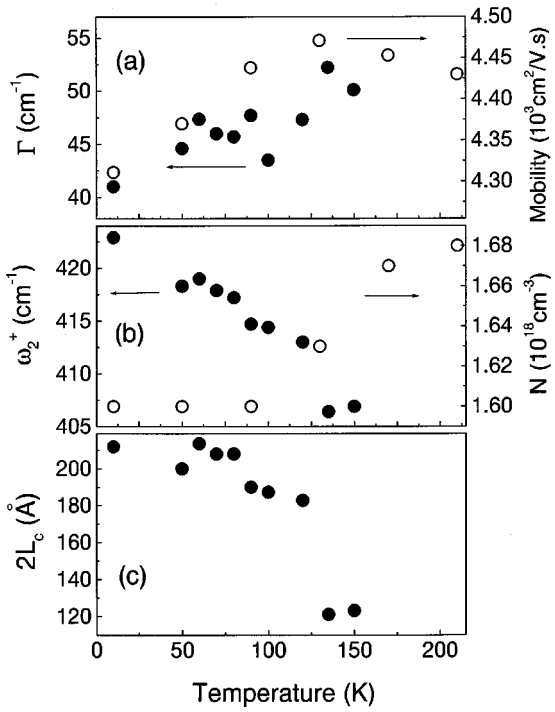

FIG. 9. Temperature dependencies of the damping constant (Γ), the frequency (ω_2^+), and the coherence length (L_c) of the AlAs-type collective plasmon-LO phonon excitations measured in the $(GaAs)_{17}(AlAs)_2$ superlattices with the electron density $N=2.5\times10^{18}\,cm^{-3}$ ($\delta=0.18$). The electron mobilities and concentrations measured by Hall effect are shown by open circles.

der the shape of the Raman line again could not be fitted with a single asymmetrical line; instead, the use of two or three such lines were indispensable in order to reproduce well the Raman line shape. This means that the coherent clusters acquired nonuniformity separating in different phases as disorder increased. The minimum and the maximum values of the parameters corresponding to these nonuniform phases are presented in Fig. 7 by closed and opened circles, respectively, while arrows point at which disorder the strong increase of the nonuniformity of the clusters was found.

It seems to be natural to analyze the effect of disorder comparing the energy of disorder Δ with the energy of the relevant collective excitations. Then, the complete screening of the disorder potential should occur at $\hbar\omega_2^+ \gg \Delta$, while in the opposite case the correlation will be frustrated by disorder. This indeed was observed in the experiment: the correlation effects (the Raman line narrowings) were found in the disordered superlattices with the ratio $\hbar\omega_2^+/\Delta \approx 5$.

C. Influence of the temperature

The effects of the temperature on the collective excitations in the disordered superlattices are shown in Figs. 8–12. As it is demonstrated in Figs. 8 and 9, the temperature almost did not influenced the AlAs-type collective excitations in the superlattices with low electron densities, while significant temperature effects were found in the highly doped ones. The redshift of the ω_2^+ frequency with the increase of the temperature was caused by the decrease of the frequency of the AlAs-type LO phonon and by the increase of the effective mass of electrons in the low and high electron density samples, respectively. The electron concentrations and the mobilities measured by Hall effect are shown in Figs. 8 and 9 as well. They did not reveal drastic alterations with the temperature as expected for the degenerated electron gas (which is the case of these superlattices).

The dependencies of the integral Raman intensities of the GaAs-type (ω_1^+) and AlAs-type (ω_2^+) modes measured in the same superlattices are plotted in Figs. 10–12. The integral intensities have a meaning of the number of collective states contributing to the Raman process. Therefore, the decrease of the integral intensity is associated with the destruction of the coherently oscillating clusters, which takes place at the critical temperature T_c.

In the superlattice with the lowest electron density ($N=7.0\times10^{17}\,cm^{-3}$) the integral intensity of the GaAs-type coupled mode revealed a strong temperature dependence, while the AlAs-type mode presented only a weak variation with the temperature. Meanwhile, in the superlattice with the higher electron concentration ($N=2.5\times10^{18}\,cm^{-3}$) the GaAs-type mode was unchanged, while the integral intensities of the AlAs-type one strongly decreased with the temperature. The integral intensity of the GaAs LO phonon line is shown in both figures as a reference; as expected it did not reveal a significant dependence on the temperature.

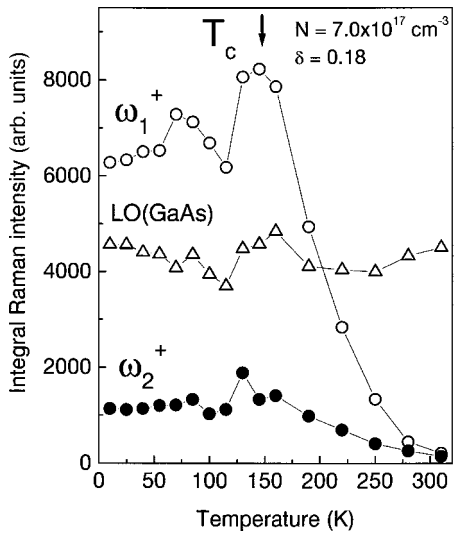

FIG. 10. Temperature dependencies of the integral intensities of the Raman lines associated with the GaAs-type ω_1^+ mode (open circles), the AlAs-type ω_2^+ mode (closed circles), and the GaAs LO phonon (opened triangles) measured in the $(GaAs)_{17}(AlAs)_2$ superlattices with the electron concentration $N=7.0\times10^{17}\,cm^{-3}$ ($\delta=0.18$).

In accordance with the results obtained in Ref. 9 the GaAs-type and the AlAs-type modes change their character with the alteration of the electron density: they have a plasmonlike and a phononlike character, respectively, in the samples with low electron densities, while the character of these modes changes completely in the high electron density limit, when the GaAs-type mode acquires a phononlike character, while the AlAs-type mode becomes mostly a plasmonlike one. This explains the different temperature effects on both the modes in differently doped superlattices: the decrease of the integral intensity with the increase of the temperature associated with the destruction of the coherent clusters, which are of electronic (not phonon) origin, takes place for that mode which has a plasmonlike character.

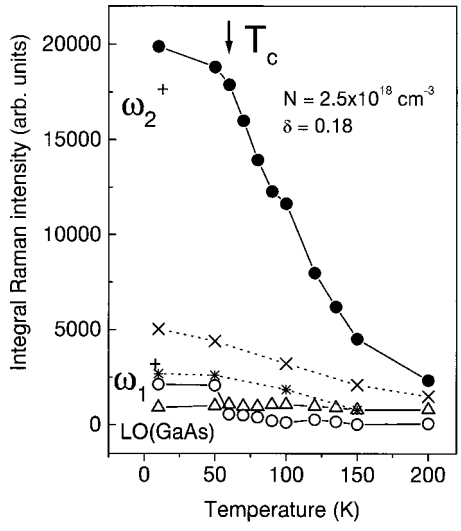

FIG. 11. Temperature dependencies of the integral intensities of the Raman lines associated with the GaAs-type ω_1^+ mode (open circles), the AlAs-type ω_2^+ mode (closed circles), and the GaAs LO phonon (opened triangles) measured in the $(GaAs)_{17}(AlAs)_2$ superlattices ($\delta=0.18$) with the electron concentration $N=2.5\times10^{18}\,cm^{-3}$. Crosses and stars show the integral intensities of the AlAs-type mode measured in the superlattices with $N=4.0\times10^{18}\,cm^{-3}$ and $N=6.0\times10^{18}\,cm^{-3}$, respectively.

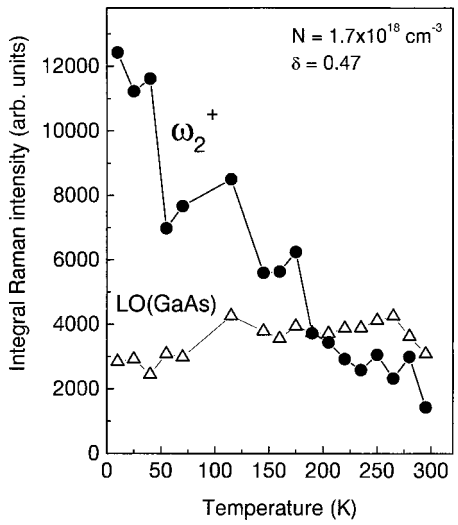

FIG. 12. Temperature dependencies of the integral intensities of the Raman lines associated with the AlAs-type ω_2^+ mode (closed circles) and the GaAs LO phonon (opened triangles) measured in the $(GaAs)_m(Al_{0.3}Ga_{0.7}As)_6$ superlattices with the electron concentration $N=1.7\times10^{18}\,cm^{-3}$ and $\delta=0.47$.

It is worth adding, that as it follows from the comparison of the data presented in Figs. 10 and 11, the critical temperature T_c depends on the doping level: the coherently oscillating clusters started to disappear at lower temperatures in the higher doped superlattices; the weakest effect of the temperature on the integral intensity was found in the superlattices with the highest doping level (shown in Fig. 11 by crosses and stars). This shows an accumulative effect of both the temperature and the disorder potential. A stronger influence of disorder on the critical temperature was observed in the intentionally disordered superlattices, where a rapid decrease of T_c with the increasing disorder parameter δ was found. As it is presented in Fig. 12, the critical temperature could not be detected already at $\delta=0.47$.

Finally, we would like to emphasize similarities between the coherently oscillating clusters observed in this study and the spontaneously polarized domains in spatially random ferroelectrics. The analogy begins with the similar asymmetrical shape of the Raman lines found in both systems, disordered doped superlattices and doped highly polarizable ferroelectric crystals. In the later case the observed asymmetry is associated with the spatial extent of the dynamic clusters responsible for the polarization. Both systems reveal similar temperature dependencies of the integrated Raman intensity showing a critical behavior (the data on ferroelectrics can be found in Ref. 15). The existence of ferroelectric order in spatially disordered dipolar materials has been recently established in Ref. 16. It was theoretically shown that despite the strong frustration present in random systems, long-range ferroelectric order is possible above a critical

electron density.[17] From this point of view, the observed abrupt alterations of the frequency and damping associated with the collective excitations could point out to the spontaneous formation of the strongly correlated dynamic clusters (in close analogy with the ferroelectric highly polarized domains), which takes place at a critical electron density in disordered superlattices. In this case, the coherence lengths (more precisely, $2L_c$) obtained here could be associated with the size of the coherent clusters. Certainly, the fundamental difference between the ferroelectric domains and the coherently oscillating clusters found in the disordered superlattices is in the parameters of the order—the electric polarization in ferroelectrics and the phase of the oscillations of the localized electrons in the disordered superlattices.

V. CONCLUSIONS

Thus, we can state that qualitative agreements with the theories[1,2,4–6] were found; however, abrupt alterations of both the damping and the line shift, which were not theoretically predicted, were indeed observed in the experiment. These abrupt changes probably evidence phase transitions in the state of the electron plasma in the disordered matter, caused by the formation of a strongly correlated plasma state in the form of coherently polarized dynamic clusters. The formation of such dynamic clusters is clearly observed in the temperature behavior of the integral intensities of the Raman lines associated with the coupled collective modes, which are proportional to the number of coherent excitations contributing to the Raman process.

To conclude, we would like to outline the mostly essential arguments testifying to the formation of the coherently oscillating clusters in the disordered superlattices. They are (i) the abrupt narrowing and redshift of the Raman lines associated with the formation of the strongly correlated collective state at a critical electron density, which returns again to the uncorrelated state with the increase of disorder, (ii) the critical temperature behavior of the integral Raman intensity pointed out to the temperature destruction of the coherent clusters, and (iii) the decrease of the critical temperature T_c with the increase of the strength of disorder (caused either by impurities or by the random variation of the layer thicknesses) attributed to the destruction of the clusters with the increasing disorder.

Based on the results obtained in the study presented here, we are able to state a scenario of the behavior of the interacting electrons in the presence of disorder. In a perfectly ordered electron system, electrons reveal the collective plasma oscillations spreading over the whole crystal in the form of plane waves. With increasing disorder at least part of the electrons form strongly correlated collective states in the form of spatial clusters, supporting the plasma oscillations. With further increase of disorder (either produced by the structural random potential or by the temperature) the coherently oscillating clusters disappear. The only single electron states forming a random electron system can be found when extremely strong disorder is attained.

ACKNOWLEDGMENTS

The financial support from FAPESP is gratefully acknowledged. We also are grateful to S. Y. Pusep for the help in the computer calculations and to A. J. Chiquito for the electrical measurements.

[1] Ph. Jacquod and D. L. Shepelyansky, Phys. Rev. Lett. **78**, 4986 (1997).
[2] P. H. Song and F. von Oppen, Phys. Rev. B **59**, 46 (1999).
[3] D. L. Shepelyansky, Phys. Rev. B **61**, 4388 (2000).
[4] C. Metzner and G. H. Döhler, Phys. Rev. B **60**, 11 005 (1999).
[5] C. Metzner and G. H. Döhler, Physica E (Amsterdam) **7**, 718 (2000).
[6] K. I. Wysokinski, Phys. Rev. B **60**, 16 376 (1999).
[7] A. Pinczuk and G. Abstreiter, in *Light Scattering in Solids V*, edited by M. Cardona and G. Güntherodt (Springer-Verlag, Berlin, 1989).
[8] Yu. A. Pusep, M. T. O. Silva, J. C. Galzerani, N. T. Moshegov, and P. Basmaji, Phys. Rev. B **58**, 10 683 (1998).
[9] Yu. A. Pusep, M. T. O. Silva, N. T. Moshegov, and J. C. Galzerani, Phys. Rev. B **61**, 4441 (2000).
[10] H. Richter, Z. P. Wang, and L. Ley, Solid State Commun. **39**, 625 (1981).
[11] F. Capasso, K. Mohammed, A. Y. Cho, R. Hall, and A. L. Hutchinson, Phys. Rev. Lett. **55**, 1152 (1985).
[12] Yu. A. Pusep and A. J. Chiquito, J. Appl. Phys. **88**, N1 (2000).
[13] Yu. A. Pusep, A. J. Chiquito, S. Mergulhão, and J. C. Galzerani, Phys. Rev. B **56**, 3892 (1997).
[14] S.-R. E. Yang and S. Das Sarma, Phys. Rev. B **37**, 10 090 (1988).
[15] P. DiAntonio, B. E. Vugmeister, J. Toulouse, and L. A. Boatner, Phys. Rev. B **47**, 5629 (1993).
[16] G. Ayton, M. J. P. Gingras, and G. N. Patey, Phys. Rev. Lett. **75**, 2360 (1995).
[17] H. Zhang and M. Widom, Phys. Rev. B **51**, 8951 (1995).